

High Gain Printed Phased Array for SAR Applications Using Planar Electromagnetic Band-Gap Technology

N. Llombart, A. Neto, G. Gerini

TNO Defence, Security and Safety, Den Haag, The Netherlands.

nuria.llombartjuan, andrea.neto, giampiero.gerini@tno.nl

ABSTRACT

This paper shows how the design of integrated arrays can significantly benefit from Planar Circularly Symmetric (PCS) Electromagnetic Band Gap (EBG) structures. Using this technology, a phased array that scans up to 40° in one dimension and that is characterized by relatively large bandwidth ($BW \approx 15\%$) is designed, manufactured and tested. The specific advantages coming from the use of PCS-EBGs are two fold. On one hand the losses associated to surface waves are significantly reduced. On the other hand each element of the array has a larger effective area that leads to a higher gain for the complete array when compared with a standard technology. Additional benefits are the low cross-polarization levels, the good front to back ratio, considering that the antenna does not include a backing reflector, and the low profile.

1. INTRODUCTION

The development of low profile array antennas for Synthetic Aperture Radar (SAR) front ends has been the subject of several recent investigations, e.g. [1], [2]. In most SAR systems the chosen solutions are scanning predominantly in one plane. The reason for this is the fact that the beam width requirements on the two orthogonal planes are significantly different. Typical requirements for SAR applications involve bandwidth (BW) larger than 10%, scanning until 45 degrees in the azimuth plane and limited scanning (≤ 15 degrees) in the elevation plane, for the aircraft roll compensation.

Different trade offs can lead to the preference of a technological solution with respect to another one. The overall cost and the complete gain are certainly important parameters. A good low cost solution could perform the limited scanning in the transverse plane mechanically and the larger scanning in the longitudinal plane electronically [3].

In this contribution we propose a technologically advanced solution for low cost, low profile and high gain front ends to be used in SAR systems. The strategy is based on the fact that the Transmit/Receive (T/R) modules are integrated on the same printed circuit boards (PCB's) that contain the antenna array elements. These elements are resonant dipoles printed on a dielectric substrate on the opposite side of the metallic plane that constitutes the ground for the micro-strip feeding lines and the T/R modules. The electromagnetic coupling between the two half spaces defined by the ground plane is achieved via resonant slots. The antenna and the T/R modules can be made completely planar. In particular, there are two significant advantages in using completely planar technology. The first is that it renders it inexpensive because of the reduced manufacturing steps. The second is that spurious radiation from the vertical connections can seriously affect the level of cross polarization. Focusing the attention on these purely planar

High Gain Printed Phased Array for SAR Applications Using Planar Electromagnetic Band-Gap Technology

structures, a useful approach is to use dense dielectric slabs in order to maximize the front to back ratio and allow the integration of the antenna with the electronic modules. With respect to this last aspect, it is well known that while compact circuit design is best achieved on high dielectric constant substrates, optimum performance printed antennas are built on low permittivity dielectrics, in order to avoid degradation of the antenna performances due to surface wave excitation. Dense and thick dielectric layers, in fact, tend to excite and support surface waves, whose control is now the key design difficulty. The advantages associated to the planarity of the structure are achieved without sacrificing the performances due to surface wave losses thanks to the use of planar circularly symmetric Electromagnetic Band Gap substrates (PCS-EBG) [4]. The key characteristics of PCS-EBGs are the following: they are simple to manufacture since they do not present vertical via holes or pins and they do present the same band gap properties for different directions of propagation. An example of 1D scanning planar array with PCS-EBG is shown in Fig. 1.

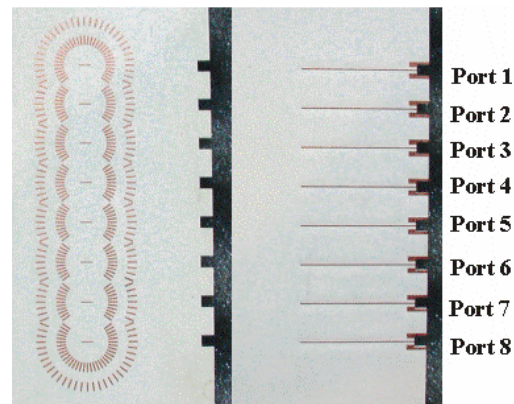


Figure 1: 1D Scanning array composed of 8 elements surrounded by PCS-EBGs (Front and back view of the prototype)

Most of the pioneering works on the use of EBG for phased arrays typically focused on the reduction of the scan blindness problem and the possibility to reduce mutual coupling between adjacent elements, [5]-[7]. On the contrary, this work aims at reducing the surface wave launched by the array elements in order to increase the gain and avoid the effects of its diffraction at the edges of the substrate.

The issue of the bandwidth achievable is one aspect to which this paper devotes particular attention with a focus on 1D scanning arrays. The feasibility of an EBG based array with BW up to 15% has actually been demonstrated with the design, manufacturing and testing of hardware bread-boards.

2. DESIGN OF ANTENNAS BASED ON PCS-EBGS

2.1 Single Antennas

The antenna considered in this section is shown in Fig. 2. It consists of two dielectric slabs with the same dielectric constant ϵ_r and different heights h and h_m divided by a ground plane. The slot etched in the ground plane is coupled to an orthogonal dipole located on the top of the upper dielectric slab h . Finally, the structure is excited via a microstrip printed on the other side of the lower dielectric slab h_m . The antenna is surrounded by a PCS-EBG consisting on two rings of radial dipoles printed on top of the upper dielectric slab.

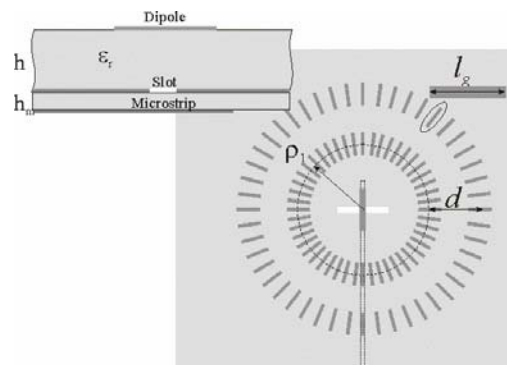


Figure 2: Topology of an array element: Slot coupled to a dipole, excited via microstrip and surrounded by a PCS-EBG

The analysis and design of single antennas surrounded by a PCS-EBG structure have been the subject of two papers [4] and [8]. In [4], the PCS-EBG concept was introduced and design guidelines were given for an optimal choice of the length of the dipoles l_g and the radial period d in order to obtain a band gap of the TM surface wave in the bandwidth of interest. Moreover, a panel with slot coupled dipoles with and without PCS-EBGs (shown in Fig.3) was built in order to measure the S-parameters between the several antennas. The radiation patterns were also measured and compared after cutting the initial panel in portions of the same dimensions (shown in Fig.4)). The antenna surrounded by PCS-EBGs showed excellent performances in terms of bandwidth (20%) and efficiency ($\approx 85-90\%$).



Figure 3: Panel with six antennas located in a square grid

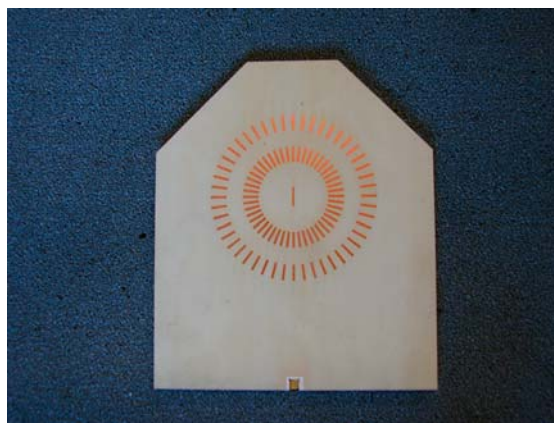


Figure 4: Panel portion containing the antenna surrounded by a PCS-EBG

In [8], a detailed explanation of the wave phenomenon that leads to the best possible theoretical performances in terms of bandwidth for single PCS-EBG antennas was given. As design guideline, the optimal radiation bandwidth (defined as the range of frequency over the antenna radiates with high efficiency) for printed antennas on grounded dense dielectric slabs ($\epsilon_r \approx 10$) and surrounded by PCS-EBGs was achieved when:

- the height of the dielectric slab at the central frequency is in the order of $0.18\lambda_d$ with λ_d the wavelength in the dielectric.
- the equivalent cavity defined by the PCS-EBG has a radius (ρ_l in Fig. 2) approximately equal to half of the TM_0 surface wave wavelength (λ_{TM0}).

2.2 Array Antennas

The PCS-EBG concept is well suited for 1D scanning arrays. The main design principle is to use linearly polarized antenna elements arrayed in the H-plane. In [4], it was demonstrated that a slot coupled dipole launches TM waves predominantly in the E-plane cut of the slab with a $\cos\phi$ angular distribution of the field intensity (Fig. 5). For this reason, one could use PCS-EBGs to reduce the TM surface waves only in a specific angular sector α , where the waves are predominantly launched, as shown in Fig. 6. For the present case, $\phi \in [-38^\circ, 38^\circ] \cup [-142^\circ, 142^\circ]$ is the angular sector where the surface propagation is blocked. Integrating the $\cos^2\phi$ power distribution over this sector, one obtains that 73% of the surface wave power is blocked. The

High Gain Printed Phased Array for SAR Applications Using Planar Electromagnetic Band-Gap Technology

angular sector concept allows closer spacing of the array elements, with respect to the cases when full rings were employed, leading to better scanning performance in the H-plane. Therefore the selection of α would be a trade-off between the free grating lobe scanning range (defined by the periodicity of the array in the H-plane) and the surface wave efficiency.

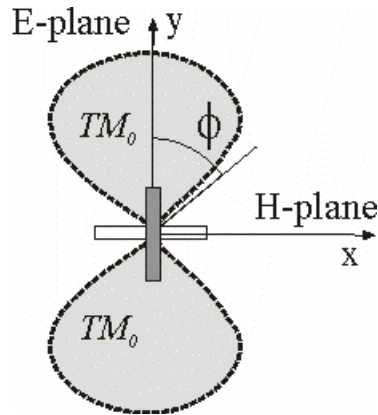


Figure 5: ϕ distribution of the TM electric surface wave field radiated by the antenna.

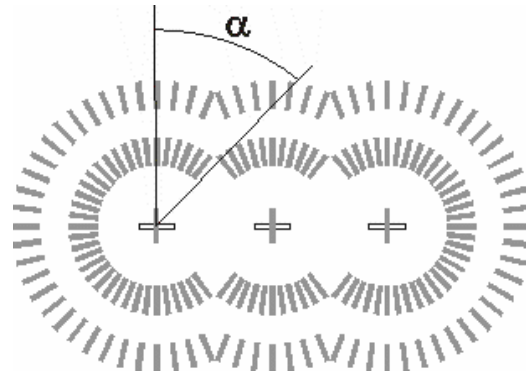


Figure 6: Reduced EBG configuration that allows arraying the elements in the H-plane.

3. X BAND ARRAY DEMONSTRATOR

An X band demonstrator composed of eight slot coupled dipoles arrayed in the H plane (Fig. 1) was designed and manufactured. The array is printed on dielectric material with $\epsilon_r = 9.8 \pm 0.245$ commercially available from Rogers. The parameters defining the EBG are the same as the ones in [1], but scaled to operate at X-band (10-12 GHz): $\rho_l = 9\text{mm}$, $d = 6.85\text{mm}$ and $l_g = 3.3\text{mm}$. The main difference is that the PCS-EBG is only present in an angular sector region α as shown in Fig. 6. All antennas are fed via 50Ω micro-strip lines of the same length connected to coaxial cables. In order to have a maximum scanning without grating lobes of 51.8° at 12 GHz, the array period is fixed to 14 mm. Once the dimension of the periodic cell and of the inner radius ρ_l is fixed, the angle α is also essentially fixed, which in the present case corresponds to $\alpha=38^\circ$.

3.1 S-parameters

First, the S-parameters of the embedded elements (single element being fed and the rest of the elements matched with a load) were measured using an HP 8510 network analyzer. A time gating procedure was used to extract the effects of the small mismatch introduced by the micro-strip-to-coax connectors (SMP adaptors). Figure 7 shows the measured and simulated reflection coefficients of the central ports and edge ports (the port numbering is given in Fig. 1). Symmetrical ports are presented in the same graphs to give an idea of the accuracy and repeatability of the measurements. For comparison reasons, the S_{11} parameter of the same array without PCS-EBG is also reported. The agreement between measurements and calculations is good besides a frequency shift that has been systematically observed in all the measured S-parameters. Such frequency shift is coherent with the tolerance in the dielectric constant. The

agreement validates the use of the MoM based commercial tool Ansoft Designer to analyze the impedance properties of these structures.

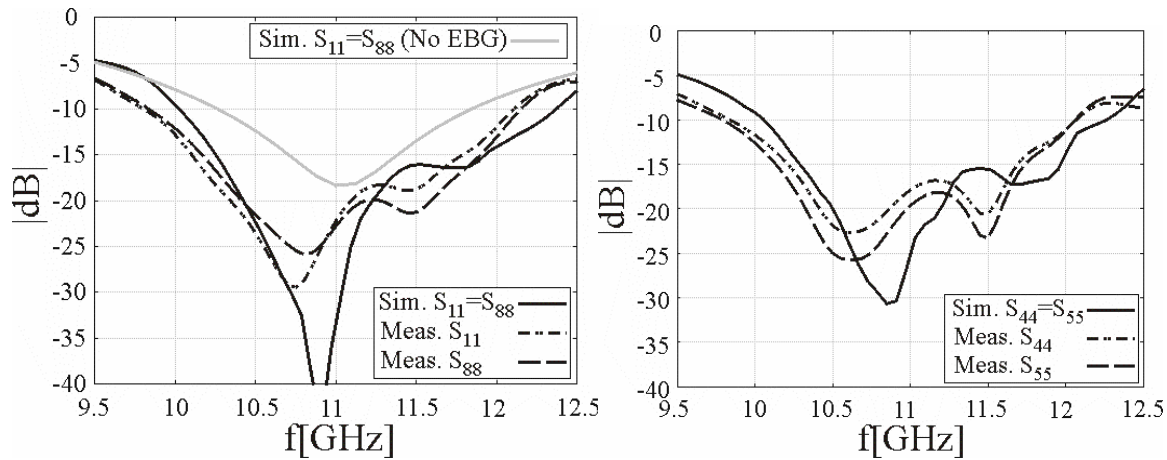


Figure 7: Measured and calculated input S-parameters for the 1D array prototype. The simulated S_{11} parameter of the same array without PCS-EBG is also shown.

For all the PCS-EBG array elements the S_{ii} parameters were lower than -10 dB over a relatively large BW (in the order of 20%). This bandwidth is larger than the case without EBGs thanks to the cavity effect created by the PCS-EBG as explained in [8].

3.2 Active Array Measurements

After having measured the S-parameters, the array was fed by means of a beam former. The beam former uses Wilkinson power dividers and manually adjustable phase shifters to obtain uniform amplitudes and linearly tapered phases in the array. The beam forming network is shown in Fig. 8.

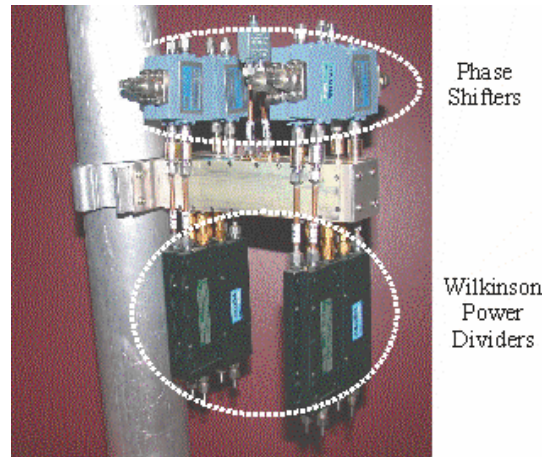


Figure 8: View of the beam former composed of Wilkinson power dividers and adjustable phase

3.2.1 Active Reflection Coefficients

The active reflection coefficients are derived as the ratio between the amplitudes of the reflected and incident waves measured using directional couplers, directly before the coaxial to micro-strip connections, see Fig. 9.

The measured active reflection coefficients of all the array elements

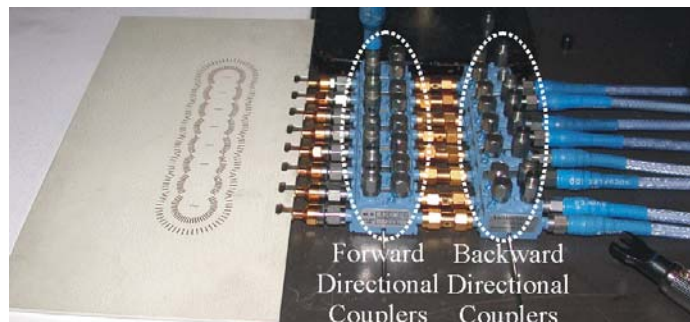


Figure 9: View of the array fed by the directional couplers (one for each signal direction) placed before the coaxial to micro-strip connections.

High Gain Printed Phased Array for SAR Applications Using Planar Electromagnetic Band-Gap Technology

are plotted in Fig. 10 as function of the frequency. The curves in the two graphs correspond to two different phase shifting conditions, associated to scanning towards $\theta = 0$ and 40 degrees at 11 GHz. Note that since the phase shift is not compensated for the deviation of the frequency from the nominal 11 GHz, the graphs are only first approximations of the reflection coefficients at actual beam scanning situations. Despite this approximation, Fig. 10 shows that the relative BW over which the array can be operated with reflection coefficients below -10 dB is in the order of 15% for both phase shifting conditions. The periodical oscillations, visible over the entire BW and for all scanning angles, are associated to standing waves due to small mismatches between the antennas and the coaxial to micro-strip connector.

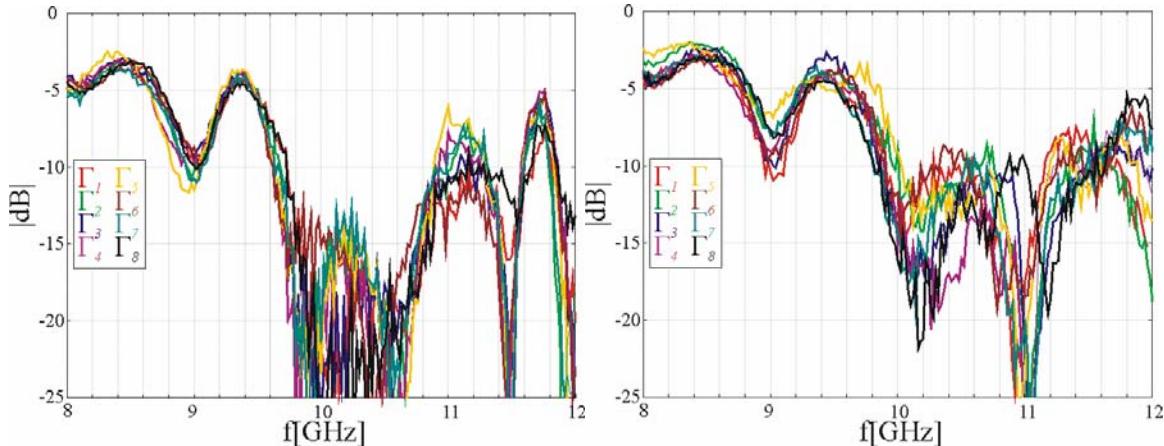


Figure 9: Measured active reflection coefficients at four different phase shifting conditions associated to scanning toward $\theta = 0$ and 40 degrees degrees at 11 GHz

3.2.1 Radiation Patterns

The radiation patterns of the array have been measured at the central frequency of 11 GHz. The co- and cross-polarized radiation patterns in the H-plane are shown in Fig. 10a for the case of broadside radiation. The patterns are normalized to their maximum value and the comparison with the results predicted by CST [9] simulations shows good agreement. The cross-polarized

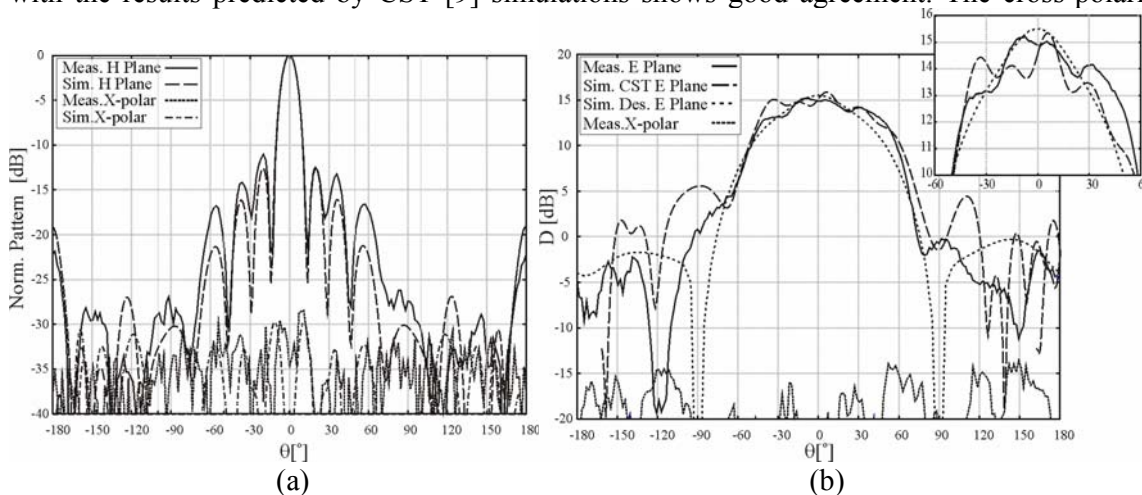


Figure 10: Measured and calculated co-polar and cross-polar normalized radiation patterns at broadside in the H- (a) and E-plane (b).

patterns are 30 dB below the co-polar radiation maximum. The E-plane co- and cross-polarized radiation patterns are shown in Fig. 10b for the case of broadside radiation. In this case, the patterns are not normalized and the values shown correspond to the measured and calculated directivities as a function of the angle. It can be seen that simulations performed via CST and measurements are fairly similar with differences that are within calculation and measurement accuracy. The actual values in both cases oscillate around the values predicted for an infinite substrate (Ansoft Designer simulations [10]). This explicitly shows that the effect of the residual surface wave diffraction is still somehow present in the E-plane. The patterns were measured only at one frequency, but it is apparent that the oscillations of the pattern around the value predicted by Designer are frequency dependent.

For scanning at $\theta = 40^\circ$, the measured co- and cross-polarized H-patterns are shown in Fig. 11a. Also the pattern simulated with Ansoft Designer is reported for comparison reasons. The beam is clean and the only noticeable aspect is that the cross polarization patterns is also maximum for $\theta = 40^\circ$. This seems to be due to surface wave diffraction contributions that for this scanning angle contribute directly to the cross-polarized pattern. The array has been also simulated with Ansoft Designer at higher frequencies. In Fig. 11b, the H-plane for $\theta = 40^\circ$ at $f = 11.6$ GHz is shown.

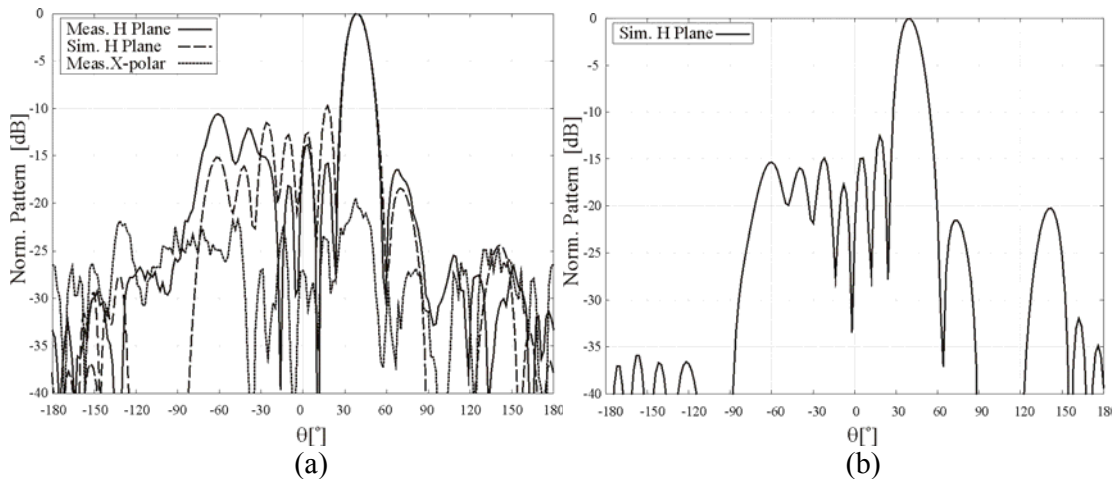


Figure 11: (a) Measured and calculated co-polar and cross-polar normalized radiation patterns at 40° scanning in the H-plane at $f = 11$ GHz. (b) Calculated patterns at $f = 11.6$ GHz.

4. COMPARISON: ARRAY WITH AND WITHOUT PCS-EBG

The two key parameters for comparison are the BW and the efficiencies of the array.

The input impedance bandwidth is larger than the case without EBGs (see Fig. 7) thanks to the cavity effect created by the PCS-EBG as explained in [2].

To visualize the surface wave propagating inside the dielectric substrate, two equivalent finite arrays, with and without the EBGs, were simulated by CST for broadside radiation. This surface wave can be clearly observed in the plot of Fig. 12a for the case without EBGs. For the case with EBGs, the plot in Fig. 12b, the shape of the surface wave fields generated by the array is qualitatively the same but the amplitude is significantly smaller. In both figures, the array

High Gain Printed Phased Array for SAR Applications Using Planar Electromagnetic Band-Gap Technology

structure has been indicated with white lines. It is evident that the EBG confines most of the fields in the cavity region. Outside the cavity the fields associated to the EBG case are about three times smaller than the ones associated to the case without EBGs. Using the results of these full wave simulations, one can estimate the surface efficiency of the arrays equal to 41% and 85%, when the array is operated with and without the EBGs, respectively.

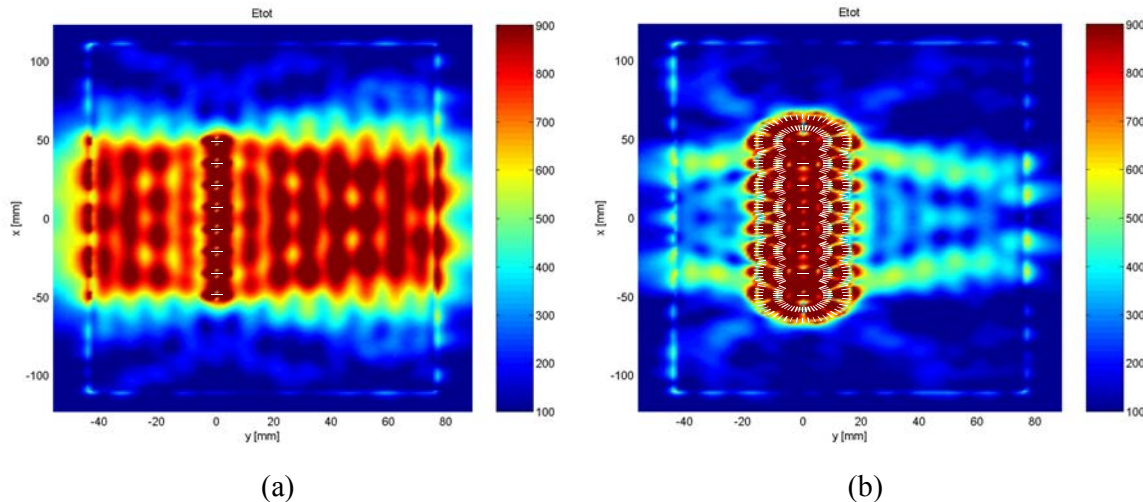


Figure 12: 2D cut of the total electric field inside the slab for $z=1\text{mm}$ with no EBGs (a) and with EBGs (b). The dimensions of the slab are $120\text{mm} \times 220\text{mm}$.

The simulated E-plane radiation pattern of the array in absence of the EBG is shown in Fig. 13 when the elements are phased to obtain a broadside beam. The curves pertinent to prediction from CST (that include edge diffraction) and the ones pertinent to Ansoft Designer (that do not include edge diffraction) are compared. One can observe that due to edge diffraction effects the two patterns are significantly different. Although the use of absorbing material to cover the edges of the finite slab would allow the reduction/suppression of these edge diffraction effects on the radiation pattern, the antenna still would be characterized by a very low efficiency of 41%. This corresponds to a gain reduction of 4 dB, which in turn corresponds to an effective antenna surface less than half of the physical one.

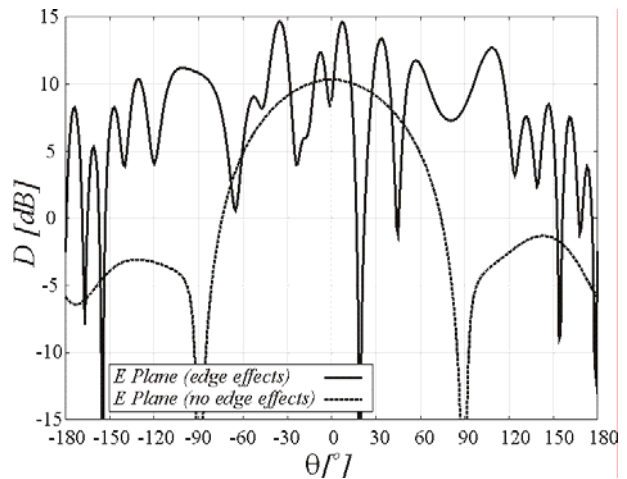


Figure 13: Simulated co-polar radiation pattern of the array in the E-plane with no EBG.

Table 1 shows the frequency behaviour of the directivity (D) and gain (G) simulated with Ansoft Designer for the array with EBGs and without EBGs. The gain is systematically lower than the directivity and the difference is a measure of the efficiency of the array. This efficiency includes both matching and surface wave losses. The simulations are done for several frequencies and scanning angles. In the case without EBGs, the gain is much lower than the directivity due to the

low surface wave efficiency. From this numbers the array appears to be well behaved over the entire frequency and angular scanning range.

	f [GHz]	10	10.5	11	11.6
Array with EBGs	$D(0^\circ)$	17,8	16,8	15,7	14,3
	$G(0^\circ)$	15,7	16	15,6	13,6
	$D(20^\circ)$	17,9	16,7	15,4	14,7
	$G(20^\circ)$	15,2	16,1	14,8	14,1
	$D(40^\circ)$	17,2	16,2	15,9	14,9
	$G(40^\circ)$	13,3	15,6	14,8	14,2

	f [GHz]	10	10.5	11	11.6
Array without EBGs	$D(0^\circ)$	14,2	13,7	15	15,3
	$G(0^\circ)$	8,8	10,2	10,4	10,8
	$D(20^\circ)$	14,7	14,6	15,3	15,3
	$G(20^\circ)$	8,7	10,6	10,3	10,7
	$D(40^\circ)$	14,7	15,1	15,3	15,4
	$G(40^\circ)$	7,9	9,4	9,2	9,4

Table 1: Simulated Directivity and Gain

5. CONCLUSIONS

Guidelines for the design of 1D scanning arrays in printed technology for SAR applications have been provided. On one side, the use of dense dielectrics improves the front to back ration and facilitates the integration of the antenna. On the other side, completely planar circular symmetric EBG technology is used to suppress the surface wave edge effects and to improve the antenna efficiency and bandwidth

A low cost and low profile array prototype has been designed manufactured and measured. The results have demonstrated the advantages pf PCS-EBG technology in terms of efficiency, bandwidth, directivity and polarization purity in one dimensional scanning arrays. The bandwidth over which a single layer and completely planar array can be scanned until 40° , without significant losses of efficiencies, has been extended to about 15%.

REFERENCES

- [1] L.L. Shafai, W.A. Chamma, M. Brakat, P.C. Strickland, G. Seguin; "Dual-Band Dual-Polarized Perforated Microstrip Antennas for SAR Applications" *IEEE Transactions on Antennas and Propagation*, Vol. 48, no. 1, pp. 58-66, January 2000.
- [2] J. Granholm, K. Woelders; "Dual Polarization Stacked Microstrip Patch Antenna Array With Very Low Cross Polarization." *IEEE Transactions on Antennas and Propagation*, Vol. 49, no. 10, pp. 1393-1402, October 2001.
- [3] P. Lacomme; "New Trends in Airborne Phased Array Radars" *Proc. IEEE Phased Array*

High Gain Printed Phased Array for SAR Applications Using Planar Electromagnetic Band-Gap Technology

Conference 2003.

[4] N. Llombart, A. Neto, G. Gerini, P. de Maagt, "Planar Circularly Symmetric EBG Structures for Reducing Surface Waves in Printed Antennas", *IEEE Transactions on Antennas and Propagation*, Vol. 53, no. 10, pp. 3210-3218, October 2005.

[5] Y. Fu, N. Yuan; "Elimination of Scan Blindness in Phased Array of Microstrip Patches Using EBG materials", *IEEE Antennas and Wireless Propagation Letters*, pp. 63-65, Vol. 3, 2004.

[6] F. Yang, Y. Rahmat-Samii, "Microstrip Antennas Integrated With EBG Structures: A low Mutual Coupling Design For Array Applications", *IEEE Transactions on Antennas and Propagation*, Vol. 51, no. 10, pp. 2936-2946, October 2003.

[7] Z. Iluz, R. Shavit, R. Bauer, "Microstrip Antenna Phased Array With Electromagnetic Bandgap Substrate" *IEEE Transactions on Antennas and Propagation*, Vol. 52, no. 6, pp. 1446-1453, June 2004.

[8] A. Neto, N. Llombart, G. Gerini, P. de Maagt, "On the Optimal Radiation Bandwidth of Printed Slot Antennas Surrounded by EBGs", *IEEE Transactions on Antennas and Propagation*, vol. 54, no. 4, pp. 1074-1083, April 2006.

[9] CST Studio Suite 2006™, Version 2006.0.0, CST GmbH.

[10] Ansoft Designer. Electromagnetically Charged EDA Software v1.1, Ansoft Corporation.

SYMPOSIA DISCUSSION – PAPER NO: 18**Author's Name: N. Llombart****Question (H. Schippers):**

- 1) What is the size of the antenna?
- 2) Are the used materials adequate for installation on an aircraft?
- 3) Are there plans for installing this MiniSAR antenna on an aircraft or UAV?

Author's Response:

- 1) The size of the dipole including two complete rings of EBG strips is 1.4 times the wavelength in free space. On X-band, this means approximately 4.2 cm. The size of the dipole depends on the wavelength in the dielectric. For 10 GHz and relative permittivity equal to 9, the size of the dipole is approximately 0.5 cm.
- 2) We suppose that the answer to this question is positive. If the antenna is used inside the wall of an airplane, an investigation should be done on which materials can best be used to give the relatively thin PCB (approximately 2.5 mm) sufficient strength. Moreover, radome issues need to be investigated.
- 3) Not at this moment.

Question (S. Sampath):

- 1) What is the dielectric constant of the material?
- 2) What is the conductor material?
- 3) What are the line widths of the conductors?

Author's Response:

- 1) Approximately 9.
- 2) Copper.
- 3) Larger than 200 micrometers.

Question:

- 1) Where is the impact of the low-cost requirement observed in the design process of the phased array?
- 2) How much cost is saved compared to conventional designs?

Author's Response:

- 1) First of all, there is no need to drill via holes or to make other vertical structures for the prevention of the propagation of surface waves.
The used EBG structures are planar, as are the antenna elements. So, only a single production step is required. In particular, when the single antenna or array are manufactured in larger quantities (for instance for wireless applications as mentioned in the presentation), this will save a substantial amount of effort and, therewith, cost. Moreover, the manufacturing of vertical structures like via holes for applications at frequencies of 60 GHz or higher is complicated and, therewith, expensive, while printing of the proposed EBG structures is relatively easy.
Another both technical and cost related aspect is that vertical structures like via holes will increase significantly the cross polarization of the antenna. If this higher level of cross polarization is unwanted, one needs to take measures to reduce the cross polarization or to apply additional filtering in the processing. These measures will of course increase cost, both in terms of man hours and in terms of



High Gain Printed Phased Array for SAR Applications Using Planar Electromagnetic Band-Gap Technology

manufacturing and material. We have shown that our solution has a very low cross polarization (see the results in the paper with a cross polarization of -30 dB).

- 2) As explained above, the cost saving aspects are both related to man hours and to manufacturing and materials. Therefore, it is hard to give numbers. Adopting a conventional planar printed design for a certain application will cost a substantial amount of work in terms of man hours needed for tuning and optimization, while to our knowledge, the performances shown in the paper (15% BW, 40 degrees of scanning and 85% of efficiency) have not yet been achieved with other planar printed designs. At this moment, we are using the technology for SAR applications, FMCW radars, and 60 GHz wireless Silicon integrated antennas, each with their own requirements in terms of design (weight / planar), BW, scanning, and/or cost.